Cyclotron Resonance in Graphite

PHILIPPE NOZIÈRES*
Bell Telephone Laboratories, Murray Hill, New Jersey
(Received October 2, 1957)

The model of the bands recently proposed by Slonczewski and Weiss for graphite single crystals is described in some detail. It is then applied to a study of the cyclotron resonance absorption in graphite, taking into account plasma effects. This theory is then compared to the recent experimental data of Galt *et al.* The comparison leads to the conclusion that the charge carriers consist of holes with effective masses ranging from $0.066m$ to $0.054m$, and electrons with effective masses from $0.054m$ to 0. The present information on the band structure of graphite is gathered in the conclusion.

I. INTRODUCTION

IN 1947, Wallace[1] published a tight-binding theory of the energy bands of graphite. He restricted his study to π electrons, taking into account only the nearest neighbor interactions. Later, more involved calculations were made by Coulson and Taylor,[2] Lomer,[3] and Corbato.[4] All of them tried to obtain the band structure quantitatively from first principles, with different approximations. Because of the very nature of the approximations involved, their results agree only qualitatively with one another.

Recently, Slonczewski and Weiss[5] (hereafter referred to as S.W.) have proposed an alternative approach. They first make a detailed group theoretical study of the crystal, thereby obtaining the "topology" of the bands. Then, since the layer spacing is large (3.37 A), they treat the interlayer interaction by perturbation theory. They are thus led to a model of the energy bands depending only on a small number of parameters. Rather than trying to calculate the latter theoretically they proposed to obtain them from experiment. In Sec. II, we sketch a somewhat altered version of their method.

The problem of fitting this model to experiment has been considered recently by McClure[6] and Hearing and Wallace.[7] McClure, using the S.W. model, gives a very detailed interpretation of the de Haas-van Alphen effect, but appears at first sight unable to account for the very large static susceptibility. The parameters he thus obtains are in fair agreement with the theoretical estimates. Hearing and Wallace propose a completely different explanation of the de Haas-van Alphen effect, which yields the correct static susceptibility. To do so, however, they have to choose values for the band parameters quite different from the theoretical estimates. In Sec. III, we propose a detailed interpretation of the cyclotron resonance data by Galt, Yager, and Dail,[8] which yields one of the parameters. In Sec. IV, we correlate this result with experimental information available from de Haas-van Alphen effect (McClure[6]), oscillatory magnetoresistance (Soule[9]), and infrared optical properties of graphite single crystals (Boyle and Nozières[10]). We then discuss the present situation with regard to the band structure of graphite near the Fermi level.

II. THE ENERGY BANDS OF GRAPHITE

Graphite has an hexagonal lattice, with layers stacked in the order 1–2–1–2 (Fig. 1). The spacing between layers is much larger than the spacing between neigh-

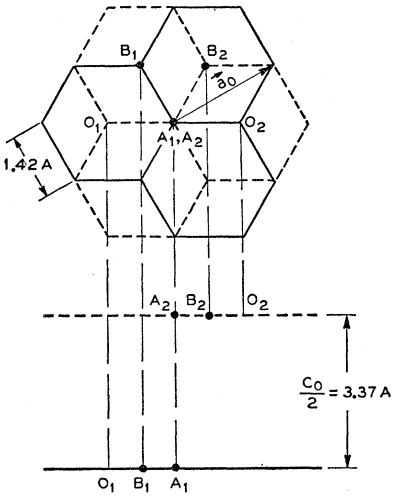

FIG. 1. The graphite lattice layer 2, represented by dashed lines, is 3.37 A above layer 1, represented by solid lines. The unit cell contains atoms A_1, A_2, B_1, B_2. The neighborhood of A_1A_2 type atoms is different from that of B_1B_2 type atoms.

* Now at the Laboratoire de Physique de l'Ecole Normale Superieure, 24 rue Lhomond, Paris V, France.

[1] P. R. Wallace, Phys. Rev. **71**, 622 (1947).

[2] C. A. Coulson and R. Taylor, Proc. Phys. Soc. (London) **A65**, 815 (1952).

[3] W. M. Lomer, Proc. Roy. Soc. (London) **A227**, 330 (1955).

[4] F. J. Corbato, Solid State and Molecular Theory Group, Massachusetts Institute of Technology Quarterly Progress Report, No. 21, 1956 (unpublished), p. 23.

[5] J. C. Slonczewski, Ph.D. thesis, Rutgers University, 1955 (unpublished). J. C. Slonczewski and P. R. Weiss, Phys, Rev. **99**, 636(A) (1955) and to be published. (Their model will be hereafter referred to as the S.W. model.)

[6] J. W. McClure, Proceedings of the Third Carbon Conference, Buffalo, New York, 1957 (unpublished); Phys. Rev. **108**, 612 (1957).

[7] R. R. Hearing and P. R. Wallace, J. Chem. Phys. Solids (to be published).

[8] Galt, Yager, and Dail, Phys. Rev. **103**, 1586 (1956).

[9] D. E. Soule, Proceedings of the Third Carbon Conference, Buffalo, New York, 1957 (unpublished).

[10] W. S. Boyle and P. Nozières (to be published).

bors in the same layer. The unit cell contains four atoms and has a height $C_0=6.74$ A. Note that the atoms belong to two classes: those which have neighbors just above them and those which do not. The Brillouin zone is a thin hexagonal prism, represented in Fig. 2.[11]

Because of the large distance between layers, it is a reasonable first approximation to neglect their interaction. We shall put this off for a moment, and consider just the single-layer problem. This problem has been studied by various authors, and we merely sketch their results. According to their behavior with respect to reflection about the layer plane, the electron eigenstates are rigorously divided into σ (symmetric) states and π (antisymmetric) states. Although the various calculations disagree on many points, they agree on one: the Fermi level (E_F) lies at the corners K and K' of the two-dimensional zone, in a π band, on a doubly degenerate level, K_3^-. At this point of the zone, the closest levels to this one are σ levels above and below E_F (Fig. 3). The distances between the latter and E_F are not known with certainty: Lomer gives a value ~ 1 ev, while Corbato proposes ~ 6 ev. Recent measurements[12] of x-ray absorption and emission of graphite both show a definite shoulder in the observed spectrum, which does not appear for diamond. These shoulders probably correspond to the above σ band edges. Because of various broadening effects, it is not possible to locate with precision the Fermi level on the x-ray spectrum, or to measure the above $\sigma-\pi$ band gaps. We can, however, assert that the latter are larger than 2 or 3 ev, thereby contradicting Lomer's result. This conclusion is consistent with that derived from photoelectric emission data.[13]

In order to obtain the energy in the neighborhood of K, we use a standard method: a change $\mathbf{k}$ in the wave vector is equivalent to a perturbation $(\hbar\mathbf{k}\cdot\mathbf{p}/m+\frac{1}{2}\hbar^2k^2/m)$ on the Hamiltonian at K. It is then straightforward to show that, to first order in k, the wave function near K is a linear combination of the eigenstates at K_3^-. There are two of these, which we will call θ and ψ. As a result, the energy surface $E(k_xk_y)$ is a circular cone with its axis along the E direction.

Since the interlayer interaction is small, we expect the above energies to be only slightly changed when we go to the actual three-dimensional crystal; the degeneracy at K_3^- will, however, be lifted, and this will result in a profound change in the shape of the bands near the Fermi level. Even though the effect is small, it will modify drastically all the properties of the electron gas. Now, since the energy shift due to the layer interaction is small, the admixture of single-layer wave functions other than θ and ψ will be small. This suggests an approximation which is the basis of the S.W. model: let us take as a wave function of the total solid a linear combination of the single-layer wave functions θ and ψ on each of the two layers in the unit cell; this leads to a fourth-degree secular equation which can readily be solved. We thus neglect the coupling of the K_3^- level with other two-dimensional levels, especially with the nearby K_1^+ and K_2^+ σ levels[14]: this may result in a slight change of the parameters entering the secular equation, which we discuss later. To sum up, the S.W. model considers a wave function of a tight-binding type for the k_z direction, and treats the change of k_x and k_y by perturbation theory.

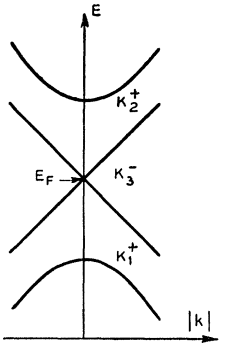

FIG. 3. The energy *vs* k_x, measured from the corner of the zone. The Fermi level lies at a doubly degenerate π level, K_3^-. The closest levels are σ levels K_1^+ and K_2^+.

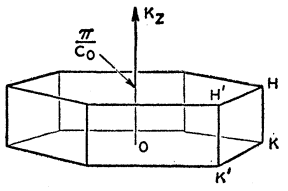

FIG. 2. Half the Brillouin zone for three-dimensional graphite (k_z ranging from 0 to π/C_0). Note that there are only two independent edges of the zone, KH and $K'H'$.

Let us sketch briefly the method used to obtain the secular equation along HK.[15] For each of the two layers of the unit cell, we consider the wave vector groups G_1 and G_2, including a set of rotations centered, respectively, at O_1 and O_2 in Fig. 1. We then consider the wave vector group G of the total crystal which includes rotations around the axis A_1A_2 eventually followed by translations along O_z. It is straightforward to express the operations of G in terms of those of either G_1 or G_2, followed by nonprimitive translations. We then define the single-layer wave functions θ_1 and ψ_1 on layer 1, θ_2 and ψ_2 on layer 2, as the basis of the same representation of G_1 and G_2 (namely the representation in which the rotations by $2\pi/3$ and $4\pi/3$ are diagonal).

The next step is to choose a value of k_z. We then can build four three-dimensional wave functions $\Phi_1(k_z)$, $\Phi_2(k_z)$, $\Psi_1(k_z)$, $\Psi_2(k_z)$ valid for any specific value of k_z, defined as

$$\begin{aligned}\Phi_1(k_z)&=\textstyle\sum_n e^{ink_zC_0}\theta_1(\mathbf{r}-n\mathbf{C}_0),\\ \Phi_2(k_z)&=\textstyle\sum_n e^{i(n+\frac{1}{2})k_zC_0}\theta_2(\mathbf{r}-n\mathbf{C}_0),\end{aligned}\tag{1}$$

[11] In what follows, we choose the z direction along the c axis of the crystal.

[12] See for instance S. Flugge, in *Handbuch der Physik* (Springer-Verlag, Berlin, 1957), Vol. 30, p. 274.

[13] E. Taft and L. Apker, Phys. Rev. **99**, 1831 (1955).

[14] The σ and π wave functions are decoupled when they lie on the same layer, but no longer so when they are on different layers.

[15] The group-theoretical techniques used in this paper are described by Bouckaert, Smoluchowski, and Wigner, Phys. Rev. **52**, 731 (1937).

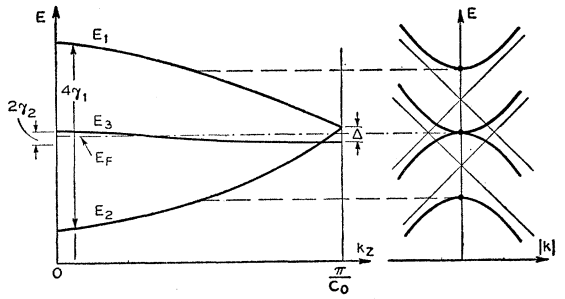

FIG. 4. The energy levels *vs* k_z along the line HK in the Brillouin zone. At right is a section of the energy surface as cut by an (E,k_x) plane for an arbitrary k_z, showing the hyperbolic shape of the bands.

and similarly for $\Psi_1(k_z)$ and $\Psi_2(k_z)$. These wave functions form the basis for a representation of G whose matrices we can form from the symmetry properties of θ and ψ. With our particular choice of θ and ψ, this representation is reduced easily into a two-dimensional representation, with basis Φ_1 and Ψ_2, and two one-dimensional representations, with basis $(1/\sqrt{2})(\Phi_2+\Psi_1)$ and $(1/\sqrt{2})(\Phi_2-\Psi_1)$ (except at $k_z=\pi/C_0$, in which case the two one-dimensional representations merge into a two-dimensional one). In this reduced representation, we may easily build the normalization matrix S and the Hamiltonian H. Each of the matrix elements is a Fourier series in $\varphi=\frac{1}{2}k_zC_0$ in which only cosine terms appear. The coefficient of 1 involves overlap of wave functions on the same layer, that of $\cos\varphi$ overlap of nearest layers, and so on: the series converges very rapidly, so that we keep only the lowest order terms. This yields the following energies along HK[16]:

$$\begin{aligned} E_1&=\Delta+2\gamma_1\cos\varphi,\\ E_2&=\Delta-2\gamma_1\cos\varphi,\\ E_3&=2\gamma_2\cos^2\varphi, \end{aligned} \tag{2}$$

(where we have chosen arbitrarily the origin of the energy scale as E_3 for $\varphi=\pi/2$). The corresponding level scheme is pictured on Fig. 4.

In order to obtain the secular equation for points of the Brillouin zone near the line HK, we must find out for each k_z the matrix of the perturbation $(\hbar\mathbf{k}\cdot\mathbf{p}/m+\frac{1}{2}\hbar^2k^2/m)$. Since it will finally turn out that the effective masses of the carriers are very small, we may neglect the term $\frac{1}{2}\hbar^2k^2/m$, and concentrate on the matrix elements of the momentum p. Furthermore, we must first make sure that the wave functions we are using are orthonormalized. In the above reduced representation, the normalization matrix may be written as

$$S=\begin{bmatrix} 1+\epsilon & 0 & 0 & 0 \\ 0 & 1-\epsilon & 0 & 0 \\ 0 & 0 & 1 & 0 \\ 0 & 0 & 0 & 1 \end{bmatrix} \begin{matrix} :\ (\Psi_1+\Phi_2)/\sqrt{2} \\ :\ (\Psi_1-\Phi_2)/\sqrt{2} \\ :\ \Phi_1 \\ :\ \Psi_2 \end{matrix}, \tag{3}$$

[16] We adopt the notation of McClure (reference 6).

in which we have limited ourselves to nearest layer interactions. We have indicated at right the labeling of rows and columns, which we shall keep in the following; $\epsilon=\langle\Psi_1|\Phi_2\rangle$ is a small quantity which we can neglect in our approximation, for it affects only the nondegenerate levels.

Using the symmetry of the wave functions, we then find easily the matrices of $\nabla_\pm=\nabla_x\pm i\nabla_y$

$$\begin{aligned} \nabla_+&=\frac{i}{\sqrt{2}}\begin{bmatrix} 0 & 0 & d_1+\delta_3^* & 0 \\ 0 & 0 & d_1-\delta_3^* & 0 \\ 0 & 0 & 0 & \delta_2 \\ \delta_3+d_1 & \delta_3-d_1 & 0 & 0 \end{bmatrix}, \\ \nabla_-&=\frac{i}{\sqrt{2}}\begin{bmatrix} 0 & 0 & 0 & d_1+\delta_3^* \\ 0 & 0 & 0 & \delta_3^*-d_1 \\ d_1+\delta_3 & d_1-\delta_3 & 0 & 0 \\ 0 & 0 & \delta_2 & 0 \end{bmatrix}, \end{aligned} \tag{4}$$

in which the constants d_1, δ_2, δ_3 are defined as

$$\begin{aligned} d_1&=\langle\Phi_1|\nabla_-|\Psi_1\rangle,\\ \delta_2&=\langle\Phi_1|\nabla_+|\Psi_2\rangle,\\ \delta_3&=\langle\Phi_1|\nabla_-|\Phi_2\rangle. \end{aligned} \tag{5}$$

The quantities d_1 and δ_2 may be shown to be real, while δ_3 is complex. In first approximation, d_1 is independent of k_z, while δ_2 and δ_3 are proportional to $\cos\varphi$, and much smaller than d_1. Since δ_3 arises as a small correction to d_1 in matrix elements connecting nondegenerate states, we may neglect it. On the other hand, δ_2, even though it is small, arises in matrix elements connecting the two components of a degenerate level: close enough to the symmetry point, these matrix elements will determine the band structure; let us therefore keep δ_2 and set it equal to $d_2\cos\varphi$.

We are now able to write down the Hamiltonian matrix for any wave vector in the neighborhood of HK. Let us describe the wave vector in cylindrical coordinates (k_z,k,α), around the axis HK. Using (2) and (4), we obtain

$$H=\begin{bmatrix} E_1 & 0 & H_{13} & H_{13}^* \\ 0 & E_2 & H_{13} & -H_{13}^* \\ H_{13}^* & H_{13}^* & E_3 & H_{33} \\ H_{13} & -H_{13} & H_{33}^* & E_3 \end{bmatrix}, \tag{6}$$

in which

$$\begin{aligned} H_{13}&=\frac{1}{\sqrt{2}}\frac{\hbar^2d_1k}{m}e^{i\alpha},\\ H_{33}&=\frac{1}{\sqrt{2}}\frac{\hbar^2d_2k}{m}e^{i\alpha}\cos\varphi. \end{aligned} \tag{7}$$

This is essentially the Hamiltonian proposed by S.W. and McClure. In determining it, we neglected several things. One is the effect of the spin-orbit splitting. S.W. have shown that this is completely negligible. More important is the coupling with the nearby σ bands. The matrix element of the Hamiltonian between π and σ wave functions involves overlap of nearest layers, and is proportional to $\sin\varphi$. This effect will therefore yield an energy shift of all the levels proportional to $\sin^2\varphi$, and will simply result in a change of γ_2 and Δ, with no further alteration of the Hamiltonian (6).

Before trying to solve the secular equation of (6), let us discuss in some detail the five parameters Δ, γ_1, γ_2, d_1, and d_2 which enter it. The parameter γ_1 corresponds to the main splitting between the singly degenerate bands, and involves overlap integrals between nearest layers. Johnston[17] estimates 0.3 ev from theoretical arguments. From a study of the magnetic properties, Hearing and Wallace[7] argue that γ_1 is of order 0.005 ev, in contradiction with the theoretical estimate. These two attitudes lead to completely different models for the energy bands, and a direct experimental measurement of γ_1 is highly desirable. Recently, Boyle and the author[10] have studied the infrared emissivity of graphite single crystals. This yields a value of γ_1 of order 0.2 ev, in accordance with theoretical estimates. In what follows, we shall assume that γ_1 is effectively of this order of magnitude.

The parameter γ_2 describes the slope of the doubly degenerate level, and determines entirely the band overlap. It arises both from the next nearest layer interaction, and from the σ-π coupling. A very rough theoretical estimate of the first effect yields a value of order 0.01 ev. The effect of the σ-π coupling depends essentially on the proximity of the σ bands. If we use the Corbato results, it is relatively weak, also of order 0.01 ev. The two effects compete, and the sign of γ_2 is doubtful. McClure's study of the de Haas-van Alphen effect yields a value of order $+0.02$ ev. Our interpretation of the cyclotron resonance data confirms this sign, while the optical properties[10] around 20μ seem to support a value of $|\gamma_2|$ of this order of magnitude.

The parameter Δ describes the separation of the two levels at $k_z=\pi/C_0$. It comes from the fact that the neighborhoods of A and B atoms are different. It also involves next-nearest-layer overlap integrals, and Carter and Krumhansl[18] estimate it to be around 0.01 ev. McClure obtains $\sim$0.02 ev, in fair agreement with the above estimate.

Our parameter d_1 describes essentially the behavior of the energy away from the line HK as we shall see later. It is related to the γ_0 of Wallace and McClure by $\gamma_0=2\hbar^2d_1/(\sqrt{3}ma_0)$, where a_0 is the primitive vector in the layer plane. (See Fig. 1.) Various theoretical estimates give values of γ_0 ranging from 1 to 4 ev. From a calculation of the magnetic susceptibility, McClure[19] obtains 2.6 ev. Using cyclotron resonance and infrared data, we obtain 2 ev.

Finally, d_2 involves matrix elements of the momentum between nearest layers, and gives rise to the anisotropy of the bands in the x, y plane. It is related to the γ_3 of McClure by $\gamma_3=2\hbar^2d_2/(\sqrt{3}ma_0)$. Johnston estimates γ_3 to be $\sim$0.1 ev. In any event it is small, and the anisotropy affects only a very narrow energy range.

Let us now turn to a study of the energy bands, and solve the secular equation (6). Since H_{33} is very small, we may neglect it for energies E such that $(E-E_3)\geq\gamma_1$. Within this approximation, (6) breaks down into two second degree secular equations. [The component $(\Phi_1e^{-i\alpha}+\Psi_2e^{i\alpha})$ of level 3 is coupled only to level 1, while $(\Phi_1e^{-i\alpha}-\Psi_2e^{i\alpha})$ is coupled only to level 2.] The energy is independent of α, given for every value of k_z by

$$E=\frac{E_1+E_3}{2}\pm\left[\left(\frac{E_1-E_3}{2}\right)^2+\frac{\hbar^4d_1^2k^2}{m^2}\right]^{\frac{1}{2}},$$
$$E=\frac{E_2+E_3}{2}\pm\left[\left(\frac{E_2-E_3}{2}\right)^2+\frac{\hbar^4d_1^2k^2}{m^2}\right]^{\frac{1}{2}}. \tag{8}$$

As Slonczewski pointed out, the surfaces $E(k_x,k_y)$ are two circular hyperboloids (Fig. 4). For k large enough, they are asymptotic to the single-layer energy cone, $E=\pm\hbar^2d_1k/m$. For k small enough, we may approximate them by paraboloids, yielding two k_z dependent effective masses $m^*(k_z)$ in any direction perpendicular to the C axis.

$$m_1^*(k_z)=\frac{m^2(E_3-E_1)}{2\hbar^2d_1^2},\quad m_2^*(k_z)=\frac{m^2(E_3-E_2)}{2\hbar^2d_1^2}. \tag{9}$$

For energies E very close to E_3, we must take into account H_{33}. But we may then use the fact that $(E_1-E_3)\gg(E-E_3)$, and solve the secular equation by perturbation theory. This gives the following energy:

$$E-E_3=\frac{\hbar^4k^2d_1^2}{2m^2}\left[\frac{(2E_3-E_1-E_2)}{(E_1-E_3)(E_2-E_3)}\right]+\frac{\hbar^2kd_2\cos\varphi}{m}\left(1+2\frac{k}{k_s}\sin3\alpha+\frac{k^2}{k_s^2}\right)^{\frac{1}{2}}, \tag{10}$$
$$k_s=\frac{2md_2(E_3-E_1)(E_3-E_2)\cos\varphi}{\hbar^2d_1^2(E_1-E_2)}.$$

Except when k_z is very close to π/C_0, one has

$$(E_3-E_2)=(E_1-E_3)=2\gamma_1\cos\varphi. \tag{11}$$

Equation (10) then simplifies, and yields the anisotropic warped energy surface shown in Fig. 5. There are four conical points, one at $k=0$, and three at $k=k_s$, at the

[17] D. F. Johnston, Proc. Roy. Soc. (London) **A227**, 349 (1955).
[18] J. L. Carter and J. A. Krumhansl, J. Chem. Phys. **21**, 2238 (1953).
[19] J. W. McClure, Phys. Rev. **104**, 666 (1956).

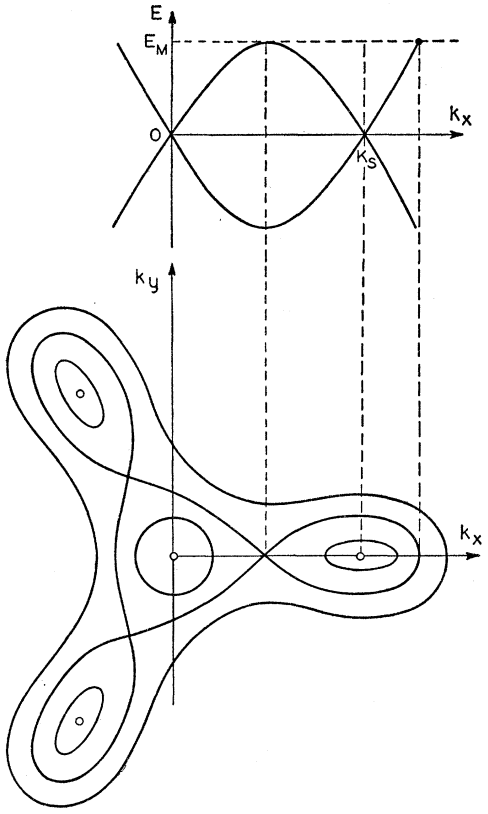

FIG. 5. The anisotropic energy surfaces near E_3, for an arbitrary k_z. The lower part shows the constant energy contours in k_x at various values of the energy while the upper part shows the function $E(k)$ in the direction $\alpha=0$. The surface $E(k_x,k_y)$ has four "feet," which merge together when E increases.

corners of an equilateral triangle. For $k\gg k_s$, the warping fades away, and the energy is again given by (8). The range of k and E in which the anisotropy is important is given by k_s and E_M (Fig. 5).

$$k_s=\frac{2md_2\gamma_1\cos^2\varphi}{\hbar^2d_1^2},\quad E_M=\frac{d_2^2}{2d_1^2}\gamma_1\cos^3\varphi. \tag{12}$$

With our present estimate of the parameters, E_M is of order 0.002 ev for $k_z=0$, which is very small. Furthermore, when $\cos\varphi$ becomes small enough that (11) might be wrong, E_M is so small that the warping is altogether negligible. In any event, the warping is a secondary feature of the bands, which may be dealt with as a perturbation upon the main band structure arising from (8).

For pure graphite, the Fermi level will be very close to E_3 (see Fig. 4), in such a way that there are an equal number of holes and electrons. Since $\gamma_1\gg\gamma_2$, the effective-mass approximation will therefore be very good near E_F except for k_z very close to π/C_0. Now, the latter range of k_z is very narrow, and furthermore yields energies rising very steeply with k_x. It therefore contains a very small number of electrons. This suggests the following approximations to the band structure near E_3: we neglect Δ, and replace the hyperbolic bands by parabolic bands with an effective mass $m^*=m^2\gamma_1\cos\varphi/(\hbar^2d_1^2)$. We furthermore neglect the warping of the bands (letting $d_2=0$). We are then left with only two parameters, γ_1/d_1^2 and γ_2. This model is completely wrong near $k_z=\pi/C_0$, where m^* goes to 0. As long as we do not deal with phenomena in which those very-low-mass carriers govern the behavior, this is nevertheless a good approximation, since it concerns only a few carriers.[20]

In this simple model, it is trivial to calculate the position of the Fermi level, the number of free carriers, etc. It is found that for pure graphite, the Fermi level crosses the level E_3 for a value of $\cos\varphi$ equal to $(\frac{2}{3})^{\frac{1}{2}}$. The total number of free carriers of each sign is in this case[21]

$$N=\frac{16}{9\sqrt{3}}\frac{m^2\gamma_1\gamma_2}{\pi^2C_0\hbar^4d_1^2}. \tag{13}$$

With the above estimates of the parameters, N turns out to be of order $10^{18}/\text{cm}^3$. If γ_2 is positive, the holes are heavier than the electrons, which as we shall see is confirmed by experiment. For energies $E\ll 2\gamma_1$, the density of states per unit energy for holes and electrons are as follows:

$$\begin{aligned}&\frac{dN_{\text{hole}}}{dE}=\frac{4m^2\gamma_1}{\pi^2C_0\hbar^4d_1^2}-\frac{dN_{\text{el}}}{dE}=\frac{4m^2\gamma_1}{\pi^2C_0\hbar^4d_1^2}f(E),\\ &f(E)=1\quad\text{if}\quad E<0.\\ &\quad=\left(1-\frac{E}{2\gamma_2}\right)^{\frac{1}{2}}\quad\text{if}\quad 0<E<2\gamma_2.\\ &\quad=0\quad\text{if}\quad E>2\gamma_2.\end{aligned} \tag{14}$$

These quantities are plotted in Fig. 6.

An important feature of the present model is that the carriers do not have *one* effective mass, but rather a continuous distribution of masses. The density of

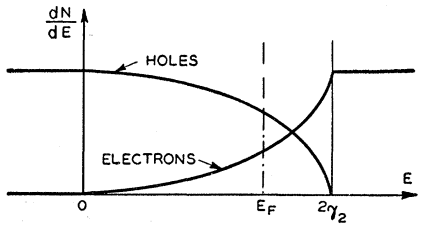

FIG. 6. The density of holes and electrons per unit energy *vs* the energy.

[20] This model would, for instance, be very bad for dealing with optical properties at energies around Δ. As was pointed out by McClure, it does not describe the diamagnetic susceptibility correctly.

[21] In evaluating (13), one must remember that there are *two* independent corners of the zone.

carriers of a given mass *vs* the mass is plotted in Fig. 7. Any model which attempts to assign discrete masses to the carriers is therefore somewhat unrealistic, although in some cases it might be a fair approximation to define an average mass for holes and for electrons, as may be seen in Fig. 7. In a certain class of experiments, such as the de Haas-van Alphen effect, or the oscillatory magnetoresistance, one only samples carriers located on the Fermi surface at points such that the cross section of the latter by a (k_xk_y) plane is maximum or minimum.[22] In the present model, this occurs at $\varphi=0$ for holes, and $\varphi=\arccos(\sqrt{2}/3)$ for electrons. The above experiments should therefore show up holes with a mass $m^2\gamma_1/(\hbar^2d_1^2)$ and electrons with a mass $\sqrt{2}m^2\gamma_1/(3\hbar^2d_1^2)$.

III. APPLICATION TO CYCLOTRON RESONANCE

In this section, we use the model of the bands developed in Sec. II to treat the problem of the cyclotron resonance in graphite single crystals. We propose an interpretation of the recent experimental data of Galt *et al.*[8] which yields a value of the mass parameter γ_1/d_1^2 in excellent agreement with that proposed by McClure. In the light of what we know about the band structure, we compare the present work with the recent explanation of Galt's results by Lax and Zeiger.[23] In what follows, we consider the geometry used by Galt, with the dc magnetic field directed along the c axis, and a circularly polarized wave propagating in the same direction.

We assume that there is no anomalous skin effect present: this point has been discussed by Lax and Zeiger, who concluded that in Galt's experiment, one is probably close to the anomalous range, but still far enough for a classical calculation to be meaningful, at least qualitatively. Let us furthermore neglect for a while possible quantum effects. It is well known[24] that under these conditions, each electron travels in k space along an "hodograph" C, characterized by constant E and k_z. Assume that this contour is closed (Fig. 8) enclosing an area $S(E,k_z)$. The time $T_c(E,k_z)$ needed for a complete revolution is then given by

$$T_c(E,k_z)=\frac{c\hbar^2}{eH}\frac{\partial S(E,k_z)}{\partial E}. \tag{15}$$

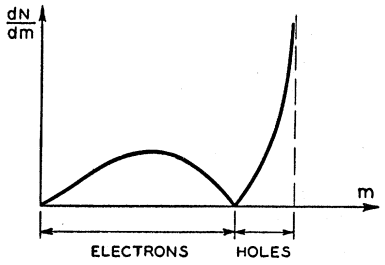

FIG. 7. A sketch of the density of carriers of a given effective mass *vs* the mass.

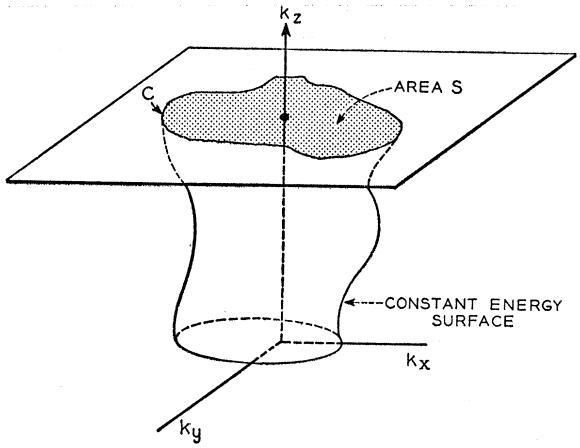

FIG. 8. In a magnetic field along O_z, each electron travels on a contour in k space like C, called the hodograph. The action variable is then proportional to the area S enclosed by C.

This classical result may be affected by two kinds of "quantum" effects. The first arises when the frequency $\omega_c(E,k_z)$ varies appreciably over an energy range of order $\hbar\omega_c(E,k_z)$, i.e., if

$$\hbar\frac{\partial\omega_c(E,k_z)}{\partial E}\geq 1. \tag{16}$$

This will occur at high magnetic fields, and will lead to resonance lines at fields H which do not depend linearly on the microwave frequency ω. Now, even when (16) is not satisfied, one may still have quantum effects arising at the touching points of two bands (as Luttinger and Kohn[25] have shown). Generally, the cyclotron level spacing is not proportional to H, except if the two touching bands are parabolic. These effects extend over an energy range of order $\hbar\omega$, in our case $\sim 10^{-4}$ ev. Now we know from Sec. II that within this distance of the touching points in k space, the energy surfaces are essentially conical. Quantum effects for such energy surfaces have been studied by McClure[19] and again they yield a nonlinear dependence between field and frequency. Galt, Yager, and Merritt[26] have performed a cyclotron resonance experiment on graphite at 24 000 Mc/sec and 72 000 Mc/sec, and they find that the absorption spreads linearly with frequency (Fig. 9). This affords experimental evidence of the absence of quantum effects of any kind in graphite, and justifies a classical treatment of cyclotron resonance.

We may then define an effective mass $m^*(E,k_z)$ for each carrier, such that $\omega_c(E,k_z)=eH/[m^*(E,k_z)c]$. This defines m^* for orbital motions of the sort relevant to cyclotron resonance. In the most general case, it does not have to be the same as the effective mass defined for other phenomena (for instance conductivity in the

[22] See, for instance, McClure, reference 6.
[23] B. Lax and H. J. Zeiger, Phys. Rev. **105**, 1466 (1957).
[24] See for instance J. W. McClure, Phys. Rev. **101**, 1042 (1956); J. M. Luttinger and R. R. Goodman, Phys. Rev. **100**, 673 (1955); Zeiger, Lax, and Dexter, Phys. Rev. **105**, 495 (1957).
[25] J. M. Luttinger and W. Kohn, Phys. Rev. **97**, 869 (1955).
[26] Galt, Yager, and Merritt, Proceedings of the Third Carbon Conference, Buffalo, New York, 1957 (unpublished).

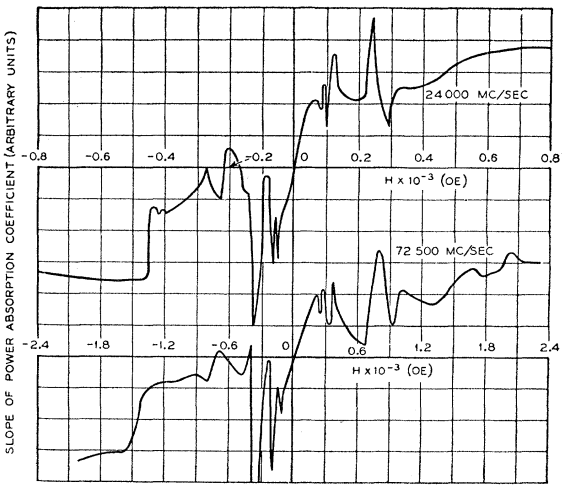

FIG. 9. The observed dP/dH plotted against H at two different microwave frequencies ω (taken from Galt *et al.*[26]). The H scale for the 72 000 Mc/sec is reduced by a factor 3, in order to emphasize the linear relation between H and ω.

xy plane). If, however, the energy contours, in the k_xk_y plane are circular, the above m^* is the same as the one occurring in the conductivity in the layer plane. Let us restrict ourselves to this simple case.

In fact, because of the exclusion principle, resonant absorption will only occur for carriers near the Fermi level E_F, so that one only samples the frequency $\omega_c(E_F,k_z)$. In the general case where ω_c varies with E, one needs a complete quantum treatment of the absorption process in order to describe correctly the observed phenoemnon. However, if ω_c is independent of E, one may neglect the exclusion principle, and perform a classical calculation of the conductivity σ of the electron gas. In our simplest model of the bands, m^* is precisely independent of E, so that the classical approach is justified.

Let us now describe any circularly polarized motion around the c axis by an algebraic frequency ω (ω and $-\omega$ corresponding to opposite circular polarizations). Let $\tau(E,k_z)$ be the relaxation time for each electron. The total conductivity of the system for a circularly polarized electric field at frequency ω is[27]

$$\sigma=\frac{1}{i}\int\frac{e^2dn(E,k_z)}{m^*(E,k_z)[\omega-i/\tau(E,k_z)]-eH/c}. \qquad (17)$$

From σ, we can easily get the complex dielectric constant, $\epsilon=1-4\pi i\sigma/\omega$. In the present case, ϵ will always be much larger than 1, giving large refraction and extinction indices. The reflection coefficient R at the surface of the sample is then given by

$$1-R\cong 4\,\mathrm{Re}(1/\sqrt{\epsilon})\cong\mathrm{Re}\left[\left(\frac{4\omega i}{\pi\sigma}\right)^{\frac{1}{2}}\right]. \qquad (18)$$

[27] For a derivation of (17), see, for instance, P. W. Anderson, Phys. Rev. **100**, 749 (1955).

$(1-R)$ measures the power loss P at the surface of the sample (through absorption and transmission), and is the quantity measured experimentally.

For high fields H, σ goes to

$$\sigma\cong(ec/iH)[n_{\mathrm{el}}-n_h],$$

where n_{el} and n_h are the total number of electrons and holes respectively.[28] If however $n_{\mathrm{el}}=n_h$, the first non-zero term of the expansion of σ is proportional to $1/H^2$. These two possibilities result in quite different behaviors of P *vs* the field H. In the first case, $P\sim\mathrm{Re}(\sqrt{H})$; the absorption curve $P(H)$ is then completely asymmetric, going to zero for one sign of H and to infinity on the other.[29] On the other hand, if $n_{\mathrm{el}}=n_h$, $P\sim|H|$, and one has a symmetric absorption curve. The experimental results show clearly that the power absorption coefficient is symmetric about $H=0$ in graphite, and we therefore conclude that in this case $n_{\mathrm{el}}=n_h$ [Fig. 1(a) of reference 8]. This conclusion is quite independent of the model chosen for the bands. This proves that the sample used by Galt was very pure, a suggestion which is confirmed by the reproducibility of the data from sample to sample, and by x-ray observations.

In order to make a really quantitative analysis of Galt's data, we should know the distribution of relaxation times, $\tau(E,k_z)$. Unhappily, this is quite outside the scope of the present study. Certainly, τ depends strongly on k_z, and probably also on E. We may, however, define an average τ for the whole group of carriers (the "majority" carriers). As was pointed out by Lax and Zeiger, the broad variation of dP/dH *vs* H suggests that, at 24 000 Mc/sec, τ is such that $\omega\tau\cong 2$. The sharp lines observed on Fig. 9 must then be due to "minority" carriers with a much longer relaxation time. Furthermore, the lines at 72 000 Mc/sec have the same fractional width as at 24 000 Mc/sec and are therefore wider as measured in oersteds (Fig. 9); this suggests that their width is not due to a relaxation process, but rather to the width of a distribution of the effective masses of the minority carriers. The following treatment will confirm this point of view. Because of the complexity of the problem with a finite τ, we shall first carry out a calculation of σ and P for $\tau=\infty$, and discuss the relevant features of the results. We then shall try to plug in to the problem some average relaxation time for the majority carriers, in order to see qualitatively how σ and P are modified by a finite τ.

Let us use the simple model described at the end of Sec. II with parabolic energy bands for any given value of k_z. It is then a straightforward matter to calculate $dn(E,k_z)$ and $m^*(E,k_z)$, and from this to calculate the

[28] As has been shown by J. A. Swanson [Phys. Rev. **99**, 1799 (1955)], the motion of carriers in high magnetic fields depends only on the topology of the bands, and not on their detailed shape. Our result for σ is just a special case of this more general treatment.

[29] The sign of H describes the orientation of the field with respect to the frequency ω of the circularly polarized electromagnetic wave.

conductivity $\sigma(H)$, using (17) with $\tau=\infty$. We obtain

$$\sigma=\frac{8e^2\gamma_2}{i\pi^2\hbar^2C_0\omega}\left[\int_0^{\varphi_0}\frac{(\cos^2\varphi-\cos^2\varphi_0)\cos\varphi}{\cos\varphi-\alpha}d\varphi+\int_{\varphi_0}^{\pi/2}\frac{(\cos^2\varphi_0-\cos^2\varphi)\cos\varphi}{\cos\varphi+\alpha}d\varphi\right], \quad (19)$$

in which α is a parameter defined as

$$\alpha=\frac{eH}{m_{\max}{}^*c\omega}=\frac{eH}{c}\frac{\hbar^2d_1{}^2}{m^2\gamma_1\omega}, \quad (20)$$

and $\varphi_0=\arccos[(\frac{2}{3})^{\frac{1}{2}}]$ is the value of $\frac{1}{2}k_zC_0$ at the point where E_F crosses the level E_3. α is simply the ratio of H to the resonant magnetic field for the holes at $\varphi=0$. The integral (19) may be calculated analytically (using principal parts when it is necessary). If we define

$$I=\sigma\frac{i\pi^2\hbar^2C_0\omega}{8e^2\gamma_2}, \quad (21)$$

we find that

$$I(\alpha)=\sin\varphi_0\cos\varphi_0+(\tfrac{1}{2}-\cos^2\varphi_0+\alpha^2)(2\varphi_0-\tfrac{1}{2}\pi)+\alpha+\frac{\alpha(\alpha^2-\cos^2\varphi_0)}{(1-\alpha^2)^{\frac{1}{2}}}\left[\ln\left(\frac{1+\alpha(1-\alpha^2)^{-\frac{1}{2}}\tan\varphi_0}{1-\alpha(1-\alpha^2)^{-\frac{1}{2}}\tan\varphi_0}\right)+\ln\left(\frac{1+(1-\alpha^2)^{\frac{1}{2}}}{\alpha}\right)\right].$$

The function $I(\alpha)$ for $\cos^2\varphi_0=\frac{2}{3}$ is plotted on Fig. 10.

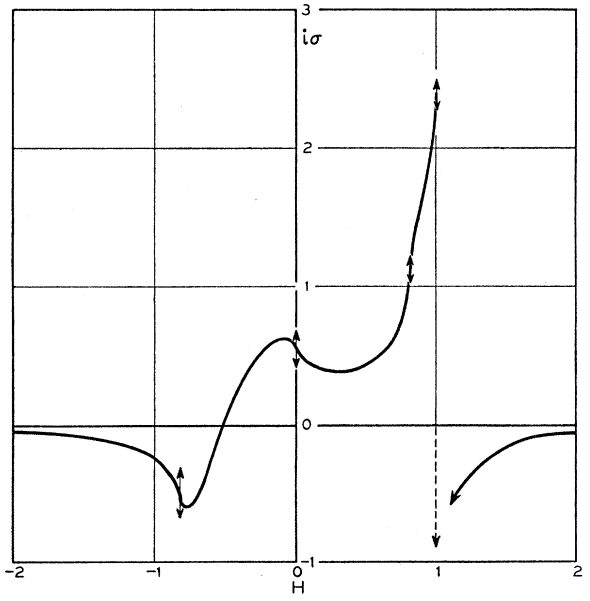

FIG. 10. The conductivity σ, times i at frequency ω for an infinite τ *vs* the magnetic field H, in suitably normalized units. [The abscissa α is equal to $(e\hbar^2d_1{}^2/cm^2\gamma_1\omega)H$, and the ordinate I is equal to $(i\pi^2\hbar^2C_0\omega/8e^2\gamma_2)\sigma$.]

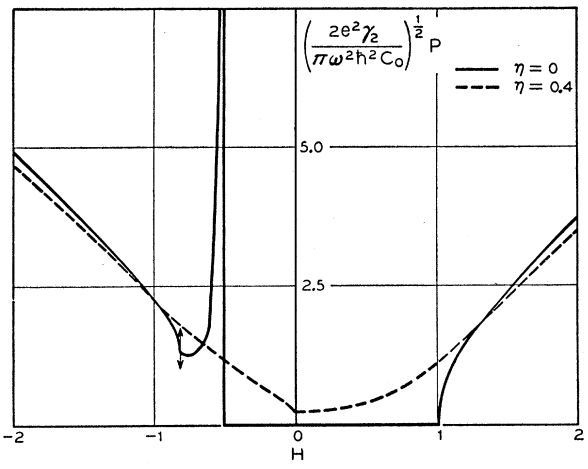

FIG. 11. The rate of power absorption P, in units of $(\pi\omega^2\hbar^2C_0/2e^2\gamma_2)^{\frac{1}{2}}$, plotted against the magnetic field H, in units of $cm^2\gamma_1\omega/e\hbar^2d_1{}^2$, for two values of the relaxation time τ, characterized by $\eta=(\omega\tau)^{-1}=0$, 0.4.

We remark that the function $I(\alpha)$ has only four singularities, at $\alpha=0, \pm\cos\varphi_0, +1$. This has a simple physical origin. We have seen that we have a continuous distribution of effective masses. If we choose a field such that some carrier in the middle of the distribution is at resonance, we do not expect any singularity in σ. The infinite negative reactance of carriers slightly lighter than those at resonance cancels the infinite positive reactance of those slightly heavier (that is what we mean by the use of principal parts). Singularities can only occur at the edge of the mass distribution: the singularity at $\alpha=1$ arises from holes with $k_z=0$, those at $\alpha=\pm\cos\varphi_0$ arise from holes and electrons at the crossing of E_3 and E_F, and that at $\alpha=0$ comes from the electrons at $k_z=\pi/C_0$. The latter is in fact spurious, being a consequence of our poor treatment of the electrons near $k_z=\pi/C_0$; those carriers do not have in fact a zero mass, and the singularity at $\alpha=0$ would disappear in a correct treatment.[30] We shall therefore disregard it.

Since we neglect the relaxation processes, the impedance σ is purely reactive and the power loss P from the cavity occurs only through transmission. Using (18) we obtain easily P, which is given by

$$P=\left[\frac{\pi\omega^2\hbar^2C_0}{2e^2\gamma_2}\right]^{\frac{1}{2}}\mathrm{Re}(-I)^{-\frac{1}{2}}. \quad (22)$$

The quantity $\mathrm{Re}(-I)^{-\frac{1}{2}}$ is plotted *vs* α on Fig. 11. We note that perfect reflection occurs in the ranges

[30] In fact, the picture is somewhat changed when one takes properly into account the splitting of the levels at $\varphi=\pi/2$. On Fig. 4, one sees that the free electron range stops at the intersection of E_F and E_2, for a value of $\cos\sigma$ equal to $\frac{1}{2}(\Delta-E_F)/\gamma_1$. One should therefore expect a very weak singularity at a very low, but nonzero, magnetic field on the electron side. This is probably smoothed because of the large E dependence of the effective mass in this range of k_z.

from $\alpha=-0.52$ to $\alpha=+1$. In this range the wave does not penetrate into the sample, and $P=0$. Because of this effect, the singularity at $\alpha=+\cos\varphi_0$ is washed out. The singularities at $\alpha=-\cos\varphi_0$ and $+1$ are still present, however. In addition, we have a new singularity at $\alpha=-0.52$. The latter cannot be assigned to any carrier in particular; it arises from the accidental fact that the conductivity goes through zero at this point.

Now consider the case in which the relaxation time is finite. The sharp singularities of $P(H)$ are then smoothed. Let us assume the same relaxation time τ for all carriers, and set $\eta=(\omega\tau)^{-1}$. The conductivity of the system is now given by

$$\sigma=\frac{8e^2\gamma_2}{i\pi^2\hbar^2C_0\omega}\frac{I(\alpha')}{I-i\eta},\quad \alpha'=\frac{\alpha}{1-i\eta},\tag{23}$$

where α and $I(\alpha)$ are defined by (20) and (21). From this, we may compute the power loss $P(H)$. The results are plotted on Fig. 11 for $\eta=0.4$. We remark that the singularity at $\alpha=-0.52$ has completely disappeared. This is always true, even for very small η, and shows that there is a fundamental difference between $\eta=0$ and η very small. We also note that the singularity at $H=0$ is not removed by the inclusion of a finite τ. Since it is in fact spurious, we may forget about it. In the range from $\alpha=-0.52$ to $\alpha=+1$ we no longer have complete reflection. Nevertheless, the penetration of the wave into the sample is smallest in this range. Any singularity superimposed on the absorption curve will be less intense in this range than outside, increasing in magnitude when η increases.

As we have mentioned, the sharp singularities observed by Galt, Yager, and Dail can only be explained if we assume minority carriers with a much longer relaxation time than that of the majority carriers. Let us therefore assume that the carriers near the crossover of E_3 and E_F (with φ very close to φ_0), have a very long τ, which, in fact, we shall take to be infinite. This assumption is plausible if the collision time is mainly determined by phonon and ionized impurity scattering. In both cases, most of the scattering will involve small changes of k_z. On one hand, there are no phonons with large k_z at helium temperature.[31] On the other, the screening in the z direction is rather inefficient, yielding a small z component of the Fermi Thomas wave vector: therefore the scattering by ionized impurities involves mostly small changes Δk_z. Now, if the change Δk_z is bound to be small, the density of states around the carriers at the cross-over is much smaller than around the other carriers, which justifies our assumption concerning the relaxation time. Under these conditions, the singularities at $\alpha=\pm\cos\varphi_0$ will not be smoothed, and will be superimposed on the smooth curve of Fig. 11. Their shape is somewhat uncertain, since they arise from a complicated complex expression. The singularity at $+\cos\varphi_0$ will be much smaller than the one at $-\cos\varphi_0$, for the reason mentioned in the preceding paragraph.

What is observed experimentally is the derivative dP/dH. This is plotted against H in Fig. 12, for $\eta=0.4$, neglecting the change due to the longer τ of the carriers at the cross over. The latter will show up as sharp singularities in the derivative curve, the one on the positive side being much less intense than the one on the negative side. At this stage, we may compare these results with the experimental data of Galt, Yager, and Dail. However, we will first discuss the resonance of minority carriers in more detail.

In deriving (23), we have neglected the warping of the energy surfaces near E_3. But the minority carriers which we are considering are precisely in the region where this warping is of importance, so that this point calls for further investigation. It turns out that it is possible to evaluate the area $S(E,k_z)$ defined in (15) for these warped bands, and thereby to calculate rigorously the cyclotron period $T_c(E,k_z)$. Let us define:

$$E-E_3=2(d_2^2/d_1^2)\gamma_1\epsilon\cos^2\varphi.\tag{24}$$

For each k_z, we must distinguish between three kinds of carriers (see Fig. 5): for $|\epsilon|<\frac{1}{4}$, we have those in the central foot of the energy surface on one part, and those in the outer feet on the other. For $|\epsilon|>\frac{1}{4}$, we have only one kind of carrier, moving along contours which have a trigonal symmetry. Using (10) and (15), we obtain $T_c(\epsilon,\varphi)$, which is given by

$$T_c(\epsilon,\varphi)=\left[\frac{2\gamma_1m^2}{\hbar^2d_1^2}\cos\varphi\right]\frac{c}{eH}g(\epsilon),\tag{25}$$

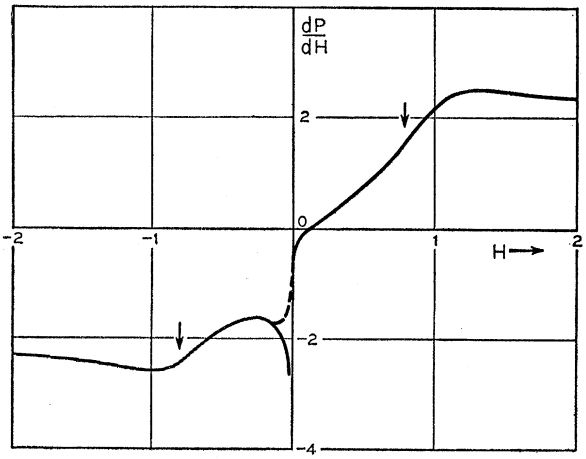

FIG. 12. The derivative dP/dH *vs* H, plotted with the same units as in Fig. 11, for $\eta=0.4$. The two arrows mark the positions of the singularities due to the minority carriers at the crossover of E_3 and E_F. To take account of the fact that the singularity at $\alpha=0$ is spurious, we indicate by a dotted line what we expect in the absence of this singularity.

[31] For an estimate of the Debye temperature along the z direction, see J. Krumhansl and H. Brooks, J. Chem. Phys. 21, 1663 (1953).

where g is a function defined for the three kinds of carriers as follows:

$$|\epsilon|<\tfrac{1}{4}: \quad g_{\text{central}}=3g_{\text{outer}}$$

$$=\frac{8\epsilon}{1+(1-16\epsilon^2)^{\frac{1}{2}}}K\left(\frac{1-(1-16\epsilon^2)^{\frac{1}{2}}}{1+(1-16\epsilon^2)^{\frac{1}{2}}}\right), \quad (26)$$

$$|\epsilon|>\tfrac{1}{4}: \quad g=\tfrac{1}{2}K/\epsilon.$$

$K(x)$ is the complete elliptic integral of the first kind. The function $g(\epsilon)$ is plotted on Fig. 13. For $\epsilon\gg\frac{1}{4}$, T_c is practically constant, equal to the period obtained when neglecting the warping. On the other hand, when $\epsilon\leq\frac{1}{4}$, T_c varies considerably, and we may wonder how to get a sharp peak from the corresponding carriers.

It is no longer possible to calculate directly the conductivity; this would require a complete knowledge of the dynamics of the carriers on the warped contours and lead to very complicated calculations. We may avoid this difficulty as follows: let us consider the carriers in a narrow energy range dE around the Fermi level E_F. They have a cyclotron period $T_c(\varphi)$ determined by (25), in which we must choose ϵ such that the energy is equal to E_F. This leads to

$$\epsilon=\frac{\gamma_2 d_1^2}{\gamma_1 d_2^2}\left(\frac{\cos^2\varphi-\cos^2\varphi_0}{\cos^3\varphi}\right). \quad (27)$$

It is possible to calculate the number dN of these carriers having a cyclotron period between T_c and T_c+dT_c. If the density dN/dT_c peaks for a certain value of T_c, we can explain the presence of sharp peaks in the spectrum.

Let us consider carriers in the neighborhood of a given contour in k space, enclosing an area S. The number of carriers in an interval $dk_z dE$ is

$$dN=(2\pi^3)^{-1}dk_z(\partial S/\partial E)dE. \quad (28)$$

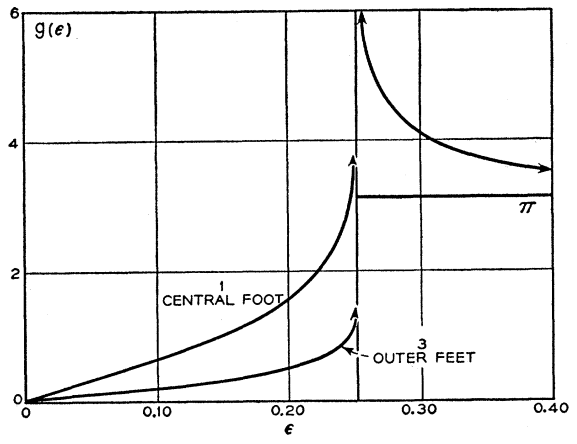

FIG. 13. The cyclotron period T_c *vs* the energy for a given value of k_z, for electrons on the warped energy surfaces near E_3. The units are defined by Eqs. (24) and (25).

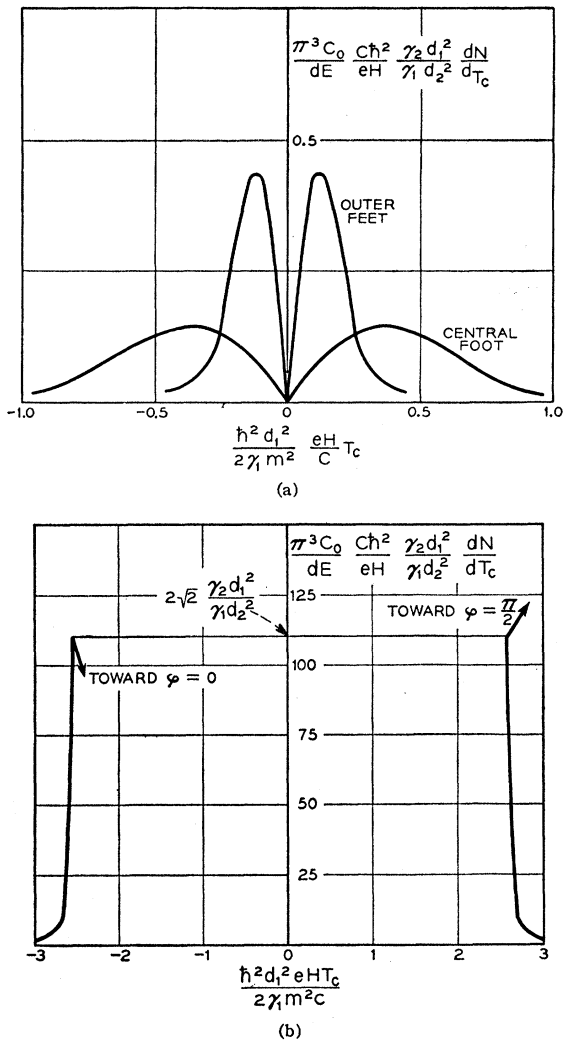

FIG. 14. The density of carriers dN/dT_c in an energy range dE around the Fermi level and resonating with the period T_c, *vs* T_c, plotted (a) for the carriers in the feet of the warped energy surfaces, (b) for the carriers outside these feet, but in the neighborhood of $\varphi=\varphi_0$. (The arrows indicate how the curve continues out of the range $\varphi\cong\varphi_0$.)

But $\partial S/\partial E$ is related to T_c by (15). We therefore obtain easily dN/dT_c as a function of φ (which we take running from 0 to $\pi/2$). The result is

$$\frac{dN}{dT_c}=\frac{2}{\pi^3 C_0}\frac{eH}{c\hbar^2}T_c\frac{d\varphi}{dT_c}dE. \quad (29)$$

Equations (25), (27), and (29) give a parametric representation of the curve of dN/dT_c *vs* T_c. In evaluating $d\varphi/dT_c$, we must remember that T_c depends on φ both directly, and indirectly through ϵ. In Fig. 14(a) we give a plot of dN/dT_c *vs* T_c, in suitable units, for the carriers lying in the feet of the energy surface. In Fig. 14(b), we give the same plot for the carriers immediately outside the feet on both the electron and the hole sides.

TABLE I. Calculated and observed fields for harmonics of minority carrier resonances.

	Harmonic	Calculated H(oe)	Observed H(oe)
Electrons	+1		−460
	+4	−115	−120
	+7	−66	−65
	+10	−46	−45
	−1	+230	+240
	−5	+92	+91
	−8	+57	+62
Holes	+1		+460
	+4	+115	+120
	−1	−230	−230

We may then draw the following conclusions: the carriers inside the feet have a very broad distribution of T_c, and very small values of dN/dT_c. They would give rise to a very weak and broad variation in the absorption, which would certainly be hidden by the broad variation due to majority carriers. On the other hand, the carriers outside the feet show a very sudden drop of dN/dT_c. The corresponding values of dN/dT_c are about 100 times larger than those of Fig. 14(a). If we neglected completely the warping of the bands, the drop would occur at the same T_c, but would be rigorously vertical. The warping just smears it slightly. Therefore, the anisotropy of the bands near E_3 does not modify at all the singularities occurring at $\alpha=\pm\cos\varphi_0$.

Although the warping does not shift or broaden the minority carrier absorption line, it has an important physical effect: it gives rise to harmonics. Because of the trigonal symmetry of the energy bands outside the feet, the motion of the carriers contains only harmonics at frequency $\omega_c(1+3n)$, where n is any integer, positive or negative. If H_0 is the field at which the fundamental resonance of minority carriers occurs, we expect to see also absorption lines at fields $H_0(1+3n)^{-1}$. Note that there would no longer be such a selection rule for the harmonics if the observed minority carriers were lying in the outer feet of the energy surface.

Let us now compare the preceding theoretical results with the experimental data of Galt, Yager, and Dail obtained at 24 000 Mc/sec (Fig. 9). The broad variation of their derivative curve agrees fairly well with the dP/dH curve of Fig. 12, for $\eta=0.4$, and therefore may be assigned to the absorption by majority carriers. One cannot ask for much more than a qualitative agreement, since our assumption of a constant τ is only approximately valid. (We must furthermore remember that we are not very far from anomalous skin effect conditions.) We have shown in Fig. 12 the position of the two discontinuities due to minority carriers, for $\alpha=\pm\cos\varphi_0$. This agrees with experiment if we choose as the fundamental singularity for $\alpha=-\cos\varphi_0$ the peak at −460 oe. We then expect a much weaker singularity at $H=+460$ oe. There is faint evidence of it on the 24 000 Mc/sec data, but it shows up better on the 72 000 Mc/sec curve.[26] The remaining lines of the observed spectrum are all ascribed to harmonics of the preceding two minority lines, as shown in Table I. We thus explain *all* the observed lines.

Furthermore, the intensity of the harmonic lines essentially depends on the penetration of the corresponding frequencies into the sample. Since the harmonics propagate by exciting an electron motion at the fundamental frequency, their penetration will depend mainly on that of the fundamental. We therefore expect the lines at −230 oe and 120 oe to be much weaker than those at 230 oe and −120 oe, which is indeed verified experimentally. The agreement between theory and experiment is therefore quite satisfactory.

Let us summarize the information on the band parameters given by this interpretation. First, the main singularity ($\alpha=-\cos\varphi_0$), occurs on the electron side. This confirms our choice of the sign of γ_2: the holes are heavier than the electrons. Furthermore, the position of this singularity yields the mass of the carriers at $\varphi=\varphi_0$

$$m^*(\varphi_0)=0.054m, \tag{30}$$

where m is the free-electron mass. From this, we get easily the maximum mass of the holes, for $\varphi=0$, which is $0.066m$. In short, the hole mass varies from $0.066m$ to $0.054m$, that of the electrons varies from $0.054m$ to 0.

It is worth mentioning that in the light of our band model, there is in fact very little choice in interpreting the data. There are so many lines in the experimental spectrum that most of them are almost certainly harmonics. But in order to have harmonics, we must have warped energy surfaces near E_F; the only place where this may occur is at the cross-over of E_3 and E_F: this fixes the nature of the minority carriers. The selection rules arising from trigonal symmetry then fixed unambiguously the choice of the fundamental line. The weak point of this interpretation is the following: the minority carriers are very few, because of the very small extent of the anisotropic region in k space. It is therefore surprising to see as large minority lines as in Fig. 9. In this respect, it must be recalled that the cyclotron resonance is a very sensitive method, especially when one uses a derivative technique. This objection is therefore not very important.

Finally, let us compare our interpretation with that of Lax and Zeiger.[23] They assume the existence of four groups of carriers: a majority and a minority hole plus a majority and a minority electron, each group having a well-defined discrete mass. They choose the same relaxation time for all carriers. Their majority carriers are taken to be 5 times as many as the minority ones. They identify the peaks at +240 oe and −120 oe with the minority holes and electrons, respectively. The peaks at +120 oe and +91 oe are then attributed to the second and third harmonics of the minority holes, those at −65 oe and −45 oe being second and third harmonics of the minority electrons. (They do not consider the possibility of negative harmonics.) From the presence

of third harmonic, they conclude that the energy surfaces around E_F cannot have trigonal symmetry. Although simple and suggestive, their analysis is purely phenomenological, and does not seem consistent with the present knowledge of the band structure of graphite. First we have seen that the distribution of effective masses was in fact continuous. Furthermore, the only region in which the bands do not have trigonal symmetry is in the outer feet of the warped energy surfaces near E_3 and we have seen that the carriers in these feet cannot give rise to sharp absorption peaks.

IV. CONCLUSION

Let us now compare these results with those obtained by other methods. From our maximum mass $0.066m$ for the holes, we can obtain the masses for holes and electrons at the section of the Fermi surface whose area is a maximum. They are respectively $0.066m$ for the holes and $0.031m$ for the electrons. These must be compared with the masses obtained from de Haas-van Alphen effect,[32] $0.070m$ and $0.036m$. The agreement here is well within the possible error in both the theory and the experiments. Recently, Soule[9] has reported similar masses derived from the oscillatory magnetoresistance. It should be noted that the ratio of the electron mass to the hole mass constitutes a check of our band model.

From the carrier masses, we obtain the parameter d_1^2/γ_1. We find it more convenient to express the result by replacing d_1 with the equivalent parameter γ_0 introduced by Wallace, defined by $\gamma_0=2\hbar^2 d_1/(\sqrt{3}ma_0)$. We then obtain

$$\gamma_0^2/\gamma_1=25 \text{ ev}, \tag{31}$$

which is just the value quoted by McClure.[6] Furthermore, note that our sign of γ_2 is also in agreement with that of McClure. As Dr. McClure has kindly pointed out to us, it would be possible in theory to obtain the parameter γ_3 (describing the anisotropy), from a study of the relative intensity of the harmonics. This, however, is a very involved calculation, and will not be attempted here.

Let us now summarize what we presently know about the band parameters. From the emissivity of graphite in the near infrared,[10] one can obtain directly γ_1 which is roughly 0.14 ev. Equation (31) then gives $\gamma_0=1.9$ ev. For γ_2 and Δ, we can take the values of McClure,[6] and we are thus led to the following model of graphite:

$$\begin{gathered}\gamma_1=+0.14 \text{ ev}, \quad \gamma_2=+0.016 \text{ ev}, \\ \Delta=+0.025 \text{ ev}, \quad \gamma_0=1.9 \text{ ev}, \quad \gamma_3=? \ (\cong 0.1 \text{ ev}).\end{gathered} \tag{32}$$

Equation (32) disagrees sharply with the values proposed by Hearing and Wallace.[7] We may point out that there are in fact two pieces of evidence which seem to contradict their model. One is the value of γ_1 obtained from infrared measurements. The other is the fact that the cyclotron absorption curve $P(H)$ supports strongly the assumption of an equal number of holes and electrons.

ACKNOWLEDGMENTS

The author wishes to thank Dr. J. K. Galt of Bell Telephone Laboratories for many useful discussions and constant encouragement, Dr. J. W. McClure for kindly communicating his results prior to publication, and Dr. C. Herring for a critical reading of the manuscript.

[32] D. Shoenberg, Trans. Roy. Soc. (London) **245**, 1 (1952).